Development 138, 227-235 (2011) doi:10.1242/dev.059683

Reconstruction of rat retinal progenitor cell lineages in vitro reveals a surprising degree of stochasticity in cell fate decisions

Francisco L. A. F. Gomes[1], Gen Zhang[2], Felix Carbonell[3], José A. Correa[4], William A. Harris[5], Benjamin D. Simons[2,6] and Michel Cayouette[1,7,8,*]

SUMMARY

In vivo cell lineage-tracing studies in the vertebrate retina have revealed that the sizes and cellular compositions of retinal clones are highly variable. It has been challenging to ascertain whether this variability reflects distinct but reproducible lineages among many different retinal progenitor cells (RPCs) or is the product of stochastic fate decisions operating within a population of more equivalent RPCs. To begin to distinguish these possibilities, we developed a method for long-term videomicroscopy to follow the lineages of rat perinatal RPCs cultured at clonal density. In such cultures, cell-cell interactions between two different clones are eliminated and the extracellular environment is kept constant, allowing us to study the cell-intrinsic potential of a given RPC. Quantitative analysis of the reconstructed lineages showed that the mode of division of RPCs is strikingly consistent with a simple stochastic pattern of behavior in which the decision to multiply or differentiate is set by fixed probabilities. The variability seen in the composition and order of cell type genesis within clones is well described by assuming that each of the four different retinal cell types generated at this stage is chosen stochastically by differentiating neurons, with relative probabilities of each type set by their abundance in the mature retina. Although a few of the many possible combinations of cell types within clones occur at frequencies that are incompatible with a fully stochastic model, our results support the notion that stochasticity has a major role during retinal development and therefore possibly in other parts of the central nervous system.

KEY WORDS: Cell fate choice, Lineage, Live imaging, Retina, Rat

INTRODUCTION

Classic experiments in the nematode *C. elegans* have shown that progenitor cells undergo stereotyped patterns of cell division to generate specific cell types at particular stages of development (Sulston and Horvitz, 1977; Sulston et al., 1983). Achieving different fates in such lineages depends on asymmetrically inherited intrinsic determinants or predictable interactions between sister cells and, consequently, mutations that affect any regulators of such components alter the lineage trees and have a major effect on cell fate decisions (Rose and Kemphues, 1998). These results indicate that lineage-dependent 'developmental programs' operate over multiple rounds of cell division and are crucial regulators of development in *C. elegans*. Similarly, in *Drosophila* neuroblasts, highly complex reproducible lineages play an essential part in neurogenesis, and their molecular mechanisms are beginning to be elucidated (Kao and Lee, 2010). Many of the cellular and molecular mechanisms at work in invertebrate lineages are also apparent in the developing vertebrate CNS, but to what extent stereotypic lineages play a part remains an open question.

Retroviral lineage tracing and single-cell dye injections in the developing cortex and retina have shown that single progenitors are multipotent and that clones vary widely in size and composition (Holt et al., 1988; Price et al., 1991; Reid et al., 1997; Turner and Cepko, 1987; Turner et al., 1990; Walsh and Cepko, 1990; Wetts and Fraser, 1988). These studies, however, did not provide information about how the clones developed over time. In an effort to tackle this problem, Temple and colleagues pioneered in vitro clonal-density cultures of cortical progenitor cells that allowed long-term time-lapse recordings that charted every cell division, death and differentiation event in the entire lineage trees (Qian et al., 1998; Qian et al., 2000; Shen et al., 2006). The order of neuronal cell production and the final cell compositions in these isolated lineages were strikingly consistent with what is known about cortical neurogenesis in vivo, suggesting that these cortical progenitors have intrinsically programmed lineages. However, detailed analysis of the lineage trees of these progenitors still showed large variability in size and composition, suggesting that stochastic decisions played a part. Indeed, a recent mathematical analysis of the cortical lineage data indicated that the distribution of lineage tree sizes is consistent with a stochastic model in which the probabilities of undergoing a division are weighted according to cell generation (Slater et al., 2009).

Although stochastic models might help to explain the variability in the number of cells within clones, understanding how specific neuronal cell types are generated at the right time within lineages of various cellular compositions is more challenging. It seems clear, however, that cortical and retinal progenitors intrinsically

[1]Cellular Neurobiology Research Unit, Institut de recherches cliniques de Montréal, Montréal, QC H2W 1R7, Canada. [2]Department of Physics, Cavendish Laboratory, J J Thomson Avenue, Cambridge CB3 0HE, UK. [3]The McConnell Brain Imaging Centre, Montreal Neurological Institute, McGill University, Montreal, QC H3A 2B4, Canada. [4]Department of Mathematics and Statistics, McGill University, Montreal, QC H3A 2K6, Canada. [5]Department of Physiology, Development and Neuroscience, University of Cambridge, Downing Street, Cambridge CB2 3DY, UK. [6]Wellcome Trust/Cancer Research UK Gurdon Institute, University of Cambridge, Tennis Court Road, Cambridge CB2 1QN, UK. [7]Département de Médecine, Université de Montréal, Montreal, QC H3T 3J7, Canada. [8]Department of Biology, Department Anatomy and Cell Biology, and Division of Experimental Medicine, McGill University, Montreal, QC H3A 1B1, Canada.

*Author for correspondence (michel.cayouette@ircm.qc.ca)

Accepted 15 November 2010

change their potential to give rise to specific cell types over time. For example, mouse cortical progenitors follow the correct sequence of neuronal cell type production, even when cultured at clonal density (Shen et al., 2006). Strikingly, mouse embryonic stem (ES) cells that are directed toward cortical fates also generate the different types of cortical neurons in the appropriate chronological order in culture (Gaspard et al., 2008). Much like in the cortex, the different cell types of the vertebrate retina are generated from progenitors in a conserved, but overlapping, chronological order (Rapaport et al., 2004; Young, 1985). The variability of the lineages generated from individual retinal progenitor cells (RPCs), combined with the temporal program of histogenesis, originally led to the suggestion that RPCs make 'lineage-independent' fate decisions based on changing environmental influences that operate at different stages of development to instruct the production of the various retinal cell types (Holt et al., 1988; Turner and Cepko, 1987; Turner et al., 1990; Wetts and Fraser, 1988). Such instructional cues, however, have not been found so far. Moreover, retinal clones generated in clonal-density cultures are, as a population, indistinguishable in size and composition from clones generated in explants of retina of the same age (Cayouette et al., 2003). Thus, RPCs seem intrinsically programmed to generate a distribution of clones of different sizes and composition, which, amazingly, when added together, generate the correct number and proportions of cell types in the retina.

There are at least two possible explanations for how RPCs generate clones of variable number and composition and yet produce a uniform retina. The first is that individual RPCs are programmed at early stages of development to generate specific and distinct lineages that when added together produce a retina. The second is that each RPC makes a set of stochastic decisions about proliferation and cellular composition in which the probabilities of each decision are structured around the overall statistics of proliferation and the fate choice that matches the population (Cayouette et al., 2006). To try to distinguish between these two models, we developed an in vitro system that allows us to reconstruct entire lineage trees of isolated rat RPCs cultured at clonal-density from embryonic day (E) 20 onwards. At this stage, RPCs generate only four cell types: amacrine (Am), bipolar (Bi), rod photoreceptor (RPh) and Müller (Mu) cells, which have overlapping histogenesis (Rapaport et al., 2004). This approach allows us to examine how RPCs choose between these alternative fates.

In this study, we address the order of cell birth within individual clones and look for signatures of stereotyped lineages. We consider whether the cell cycle time or number of RPC divisions is predictive of cell fate. We determine whether there are fate-committed precursor cells in the developing retina. Finally, we explore the statistical features of the lineages to determine whether the overall characteristics of the assemblage of clones may be determined by simple rules. By drawing together these observations, we propose a model of retinogenesis in which stochastic decisions play a major part.

MATERIALS AND METHODS

Retinal progenitor cell culture and time-lapse imaging

Retinal cells from E20 Sprague Dawley rat retinas were cultured as described (Cayouette et al., 2003). The dissociated cells were allowed to settle for a few hours in a CO_2 incubator at 37°C before they were placed under the time-lapse microscope. A total of 90-110 RPCs were selected in each experiment and imaged using a Hamamatsu CCD video camera connected to a computer equipped with Volocity software (Perkin Elmer) programmed to capture a frame every 5 minutes for a period of 9-14 days. The cells were kept in a 37°C, 8% CO_2, 12% O_2 environment.

Immunostaining

After the recording, the cells were fixed with 4% paraformaldehyde for 10 minutes and the following antibodies were used for immunostaining: monoclonal mouse anti-Islet1 (1:2000; produced by T. Jessell and obtained from the Developmental Studies Hybridoma Bank) and rabbit anti-Pax6 (1:10,000; Santa Cruz Biotech). Primary antibodies were detected using goat anti-mouse IgG2b Alexa Fluor 488 and goat anti-rabbit IgG Alexa Fluor 594. In all cases, nuclei were stained with Hoechst 33342.

Reconstruction of RPC lineage trees

For lineage tree reconstructions, the time-lapse movies were replayed and the movement and divisions of each individual RPC were followed manually over time. To generate the lineage tree, the progenies of a single cell were tracked and their fates were identified based on their specific morphologies and validated by the corresponding immunostaining data.

Numerical simulation of the RPC lineage trees

The clone size distribution and lineage composition predicted by the stochastic models discussed in the text were determined by numerical simulation using a Monte Carlo analysis based on the Gillespie algorithm (Gillespie, 1977). The balance between proliferation and differentiation, and the specification of the different differentiated cell types, were set by fixed probabilities as defined in the main text. Where necessary, the distribution of cell cycle times was taken to be log-normal with an average and variance fixed by the fit to the experimental data as defined in the main text.

RESULTS

Cell type identification and lineage reconstruction

To study retinal lineages, we cultured E20 rat RPCs at clonal density and recorded their development over time using long-term time-lapse microscopy. In such cultures, RPCs had elongated cell bodies, lacked neurites, appeared phase-dark and were highly motile (Fig. 1A and see Movie 1 in the supplementary material). By contrast, differentiated cells were usually phase-bright, displayed thin processes and were largely immotile. Retrospective analysis confirmed that more than 80% of the cells selected at the beginning of the experiment were RPCs, as they later divided and gave rise to neurons.

We conducted 25 independent experiments over a period of more than 2 years and followed the fate of 2347 RPCs. Of these, 856 were excluded from further analysis because the RPC either died (6.3%), moved away from the field of view (2.7%), touched another cell that was not part of the clone (6.5%), or immediately differentiated without dividing (21%). As a result, we recovered a total of 1491 RPCs that divided at least once to generate clones containing two cells or more. After time-lapse recording, we fixed and stained the cells for Pax6, Islet1 and with Hoechst. As we previously reported (Cayouette et al., 2003; Cohen et al., 2010), using a combination of cell morphology and expression of Pax6 and Islet1, we were able to identify the four major retinal cell types expected to be generated from perinatal RPCs: Am, RPh, Bi and Mu (Fig. 1B-I). With the staining data in hand, we then retrospectively reconstructed the lineage trees containing three or more cells by playing back the video recordings frame by frame and mapping the birth order of the different cells within the lineage (Fig. 1E). From the 1491 RPCs, 1211 were recorded to have undergone a terminal division that generated two differentiating daughters, but were not further analyzed in terms of cell type composition because they did not provide any additional information compared with studying fixed samples, as undertaken

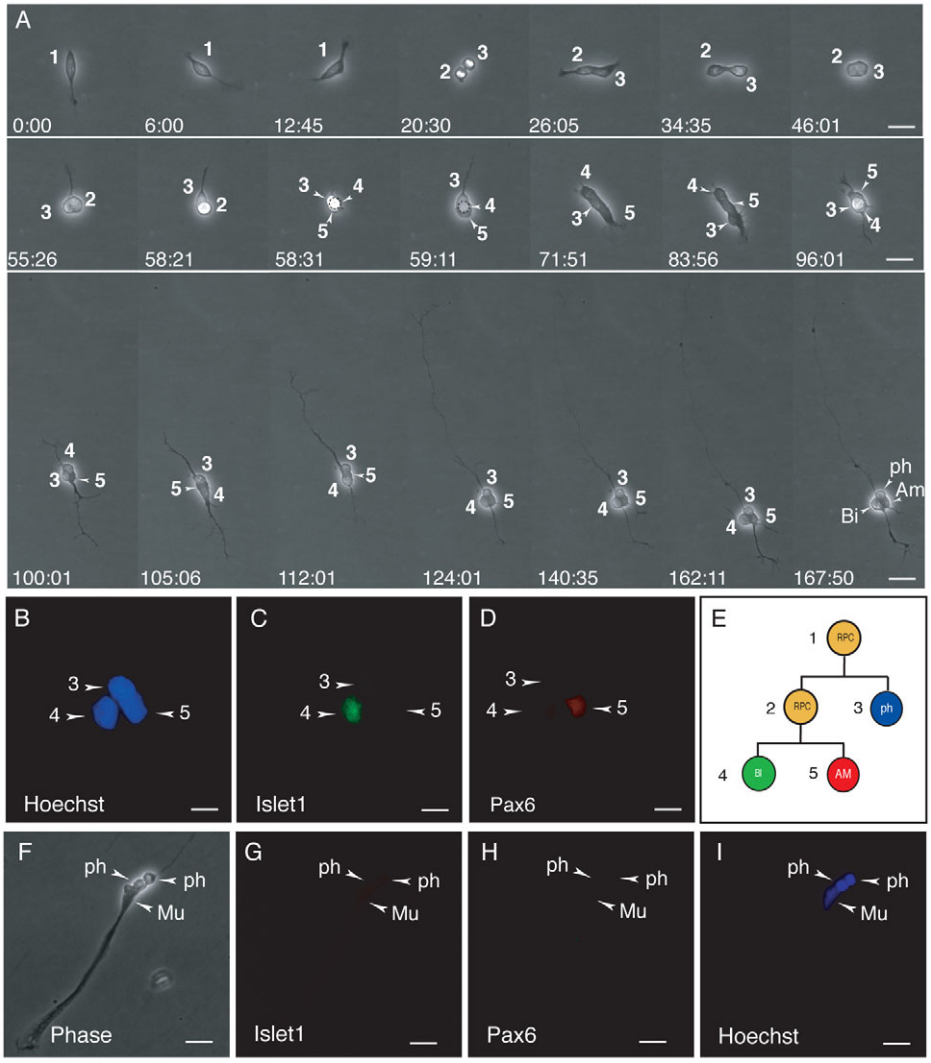

Fig. 1. Lineage reconstruction and cell type identification. (**A**) Snapshots of a time-lapse video showing a rat retinal progenitor cell (RPC) undergoing a P/D division (*t*=20:30) and a terminal D/D division (*t*=58:11) giving rise to a three-cell clone composed of an amacrine (Am), a bipolar (Bi) and a rod photoreceptor (RPh or ph) cell. Time is given in hours:minutes. (**B-D**) Retinal cell type identification in the clone recorded in A. In this clone, cell 4 stained for Islet1 and cell 5 stained for Pax6, identifying them as Bi and Am, respectively. The remaining cell was negative for both markers and displayed typical RPh cell morphology with a small round cell body and simple processes and showed characteristic Hoechst staining. (**E**) Based on the staining data in B-D and the videomicroscopy in A, the lineage tree of this clone was reconstructed. (**F-I**) A clone containing two RPh cells and one Müller glial cell (Mu; Pax6 negative and Islet1 negative) with distinct glial morphology, large nucleus, absence of neurites and lack of expression of neuronal markers. Scale bars: 20 μm in A; 8 μm in B-D; 20 μm in F-I.

previously (Cayouette et al., 2003). Of the remaining 280 RPCs that divided more than once, the lineage trees of 129 could be reconstructed (all reconstructed lineages leading to clones of three or more cells are shown in Figs S1-S5 in the supplementary material), whereas the remaining clones had cells that were lost during the fixation and immunostaining process, or the outcome of at least one mitosis could not be resolved, most often owing to cells moving on top of each other.

In the successfully reconstructed lineages, there were 465 differentiated cells, three of which had an unidentified fate (0.6%), and in the remaining cells we found 341 RPh (73.8%), 59 Bi (12.8%), 49 Am (10.6%) and 13 Mu (2.8%). These proportions are similar to those obtained after labeling RPCs at postnatal day (P) 0 with retroviral vectors in the mouse retina (Turner et al., 1990).

The mode of cell division in RPCs is stochastic

Using the reconstructed lineage data, we first asked how E20 RPCs achieve the required balance between proliferation and differentiation. We analyzed the different modes of cell division observed in the overall population. For the ensemble of clones with three or more cells, for which the lineage trees were fully reconstructed, the first division must inevitably involve the survival of at least one progenitor. Therefore, to obtain an unbiased statistical measure of the modes of cell division, we examined the lineage trees of the clones with three or more cells after their first division. Out of 199 divisions recorded, 44 (22.1%) were self-renewing divisions that produced an RPC and a differentiating daughter (P/D divisions), whereas 144 (72.4%) were terminal, giving rise to two differentiating daughter cells (D/D divisions). Such terminal divisions, although symmetric in the sense that both daughters exit the cell cycle, could also be symmetric or asymmetric in the sense that the daughter cells may be of the same or different types, respectively (Cayouette et al., 2006). To avoid confusion, we shall generally refer to all terminal divisions as D/D divisions, regardless of whether the two daughter cells adopt the same or different fates. Finally, only 11 divisions (5.5%) were found to generate two RPCs (P/P divisions). Since the P/P mode of division accounts for only a small fraction, these results indicate that differentiative (D/D) divisions, and to a lesser extent self-renewing (P/D) divisions, are the major source of neurogenesis and gliogenesis in the perinatal retina, at least in culture.

Although these figures point unambiguously to the predominance of D/D and P/D divisions at this stage of retinogenesis, they leave open the question of whether the balance of these division modes changes significantly over the timecourse of the experiment. To investigate this, we compared the second divisions of each lineage tree with those of the third and beyond. Of the 131 second divisions, 95 were D/D

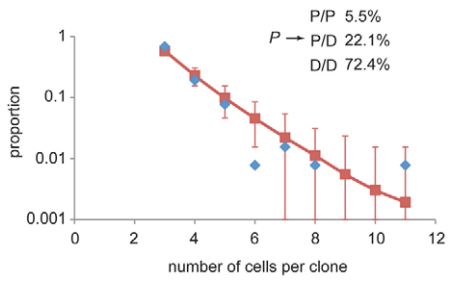

Fig. 2. The observed clone size distribution is reproduced by a stochastic model. The data points (blue) show the size distribution associated with the 129 clones with three or more cells. If we assume that the balance between proliferation and differentiation is determined stochastically, with RPCs dividing with a fixed probability P_{PP}=0.055 of adopting P/P cell fate, P_{PD}=0.221 of adopting P/D cell fate, and P_{DD}=0.724 of adopting D/D cell fate, we obtain the clone size distribution given by the red curve. The error bars on the theoretical curve denote 95% confidence intervals and are a result of the finite sample size. Since the probability of adopting the P/P cell fate is small, the size distribution is close to exponential, reflecting the fact that the majority of clones can be described by a sequence of asymmetric P/D divisions terminating in a D/D division.

(72.5±7.4%), 31 were P/D (23.6±4.3%) and five were P/P (3.8±1.7%); errors are estimates based on Poisson statistics for the counts, i.e. (count±$\sqrt{}$count)/total counts × 100%. This leaves 68 third and beyond divisions, of which 49 were D/D (72.1±10.3%), 13 were P/D (19.1±5.3%) and six were P/P (8.7±3.6%). The difference between the second and third divisions remains within the error bars, indicating that over the timecourse of the experiment the ratio of D/D, P/D and P/P divisions remains roughly constant.

The similarity in the relative division ratios between one generation and the next suggests that the balance between proliferation and differentiation of a RPC is not influenced by the fate of its parent. In other words, the division mode of a given RPC (P/P, P/D or D/D) is unpredictable and, in this sense, stochastic. To test this possibility directly, we compared the chance of finding a clone of size n in the experimental dataset with that predicted by a model in which RPCs divide with a fixed probability P_{PP}=0.055 of adopting the P/P cell fate, P_{PD}=0.221 of adopting the P/D cell fate and P_{DD}=0.724 of adopting the D/D cell fate (Fig. 2). Strikingly, the results of a numerical simulation (see Materials and methods) show an excellent agreement with the experimental data. Moreover, for the same number of clones with three or more cells (129), the model predicts an approximately normal distribution for the total number of cells across all clones, with an average of 487 and a standard deviation of 22. This is again consistent with the 465 observed in the experiment.

These results suggest that, at least from E20 and over the timecourse of the experiment in vitro, the mode of division of RPCs is stochastic with biased probabilities that remain approximately fixed. Our previous findings that the size distribution of clones that develop in clonal-density cultures is very similar to that of clones that develop ex vivo in retinal explants (Cayouette et al., 2003) suggest that this is not a pathology associated with culture conditions. In addition, because the RPCs are cultured at clonal density, these results suggest that biased probabilities do not depend on specific environmental cues.

The order of cell birth varies within retinal lineages

Having established that a stochastic mode of division can explain the size and shape of our retinal lineages, we next focused on the cell type distribution within these lineages. Many previous cell birthdating experiments in vivo have indicated that, at the population level, retinal cell type production follows a rough chronological order (Rapaport et al., 2004; Young, 1985). Similarly, we previously reported that the general chronology of cell type production observed in vivo is reproduced in clonal-density cultures (Cayouette et al., 2003), suggesting that the timing mechanisms controlling retinal cell birth order are maintained in isolated cells in culture. In these previous studies, however, the order of cell birth was analyzed with respect to the overall cell population. Here we tested whether the general order of retinal cell type production is achieved through a temporal program encoded within each retinal lineage.

To define birth order, we looked at lineages containing two or more cell types (n=71) using a pairwise comparison. For each reference cell generated in a lineage, we determined how many times a different sibling cell type was produced after that reference cell in the same lineage (Table 1). Surprisingly, we found violations of the general order of cell birth within individual lineages. In some cases, for example, a Bi cell was generated before an Am cell, whereas in others the opposite was true; and although Mu cells tended to be generated at the end of their lineage trees, in two cases out of 13 clones we found that photoreceptors were produced after a Mu cell (Fig. 3). This suggest that RPCs do not lose their neurogenic potential once they have generated a glial cell, which might be a particularity of retinal lineages compared, for example, with cortical lineages (Qian et al., 2000; Shen et al., 2006). These results suggest that the order of retinal cell type production is not strictly encoded in each lineage, at least not from E20 onwards in culture.

Cell cycle time is uncorrelated with cell fate choice or mode of division but its variability helps predict the termination of retinogenesis

We next considered whether the time that an RPC spends in the cell cycle correlates with cell fate choice. We directly measured the cell cycle time of RPCs generating all observed combinations of

Table 1. A pairwise comparison matrix of cell birth within RPC lineages

		Comparison cell			
		Am	RPh	Bi	Mu
Reference cell	Am (15)	×	13	5	4
	RPh (37)	20	×	19	9
	Bi (24)	13	15	×	5
	Mu (02)	0	2	0	×

This analysis demonstrates that the order of retinal cell birth is highly irregular within lineages. An arbitrary order of cell birth was chosen based on the peak production time of each cell type observed in vivo: amacrine (Am), rod photoreceptor (RPh), bipolar (Bi) and Müller (Mu). This order, however, has to be taken cautiously as it is known that the sequence of retinal cell type production is overlapping in vivo. Similarly, we found that Am, Bi and RPh birthdates in culture largely overlap (not shown). Each reference cell type was assessed in all clones and the cell type produced after that event (comparison cell) was determined. The gray-shaded boxes show the number of violations to the order. This matrix shows, for example, that in 15 events when an Am cell was generated, 13 Rph, five Bi and four Mu cells were born after the Am cell. Also, in 24 cases when a Bi cell was generated, five Mu were generated after, as expected; however, 15 RPh and 13 Am cells were also born after the Bi cell in the lineage. Only the genesis of Mu cells appears to be roughly fixed, although in two cases when a Mu was born, two RPh (in two different clones) were generated after. No Bi or Am cells were ever generated after the birth of a Mu cell (in 11 events of Mu genesis, not shown).

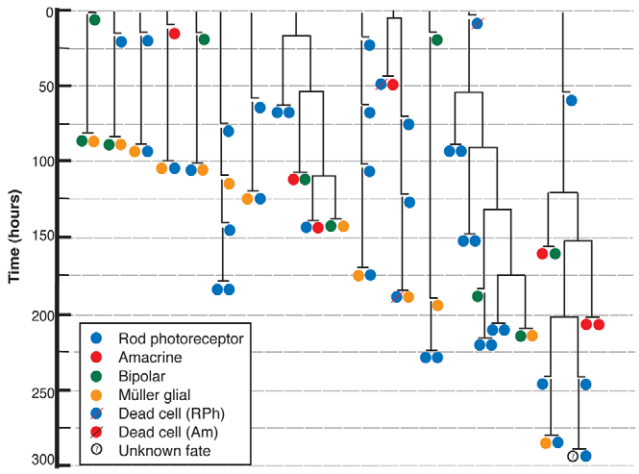

Fig. 3. Müller cell-containing clones. The lineage trees of all Mu-containing clones were reconstructed. Note that with the exception of two lineages, the Mu cells are generated at the end of the lineage. Note also that only a single Mu cell is present in any lineage.

daughter cell pairs by counting the elapsed time between the mitosis that produced these cell pairs and the previous one. We found no significant difference in cell cycle time of divisions producing any of the combinations observed (Fig. 4A), indicating that cell cycle time does not correlate with any particular cell fate decision. Previous birthdating studies in vivo showed that the average cell cycle time of the RPC population increases as development proceeds. Since lineage-terminating divisions are more common at postnatal stages, we tested the idea that longer cell cycles might constitute a cue for terminal divisions, and hence lineage termination. However, we found no differences in the average cell cycle time between P/P, P/D and D/D divisions (Fig. 4B). Although the average cell cycle time did not differ significantly for the different modes of division, it remained possible that the relative cell cycle time of two sister RPCs proliferating in the same lineage could differ according to their mode of division. To test this, we compared the cell cycle time of sister RPCs in which one had undergone a P/P division whereas the other had undergone a differentiative division (P/D or D/D), and found no consistent trend for longer or shorter cell cycle times (Fig. 4C). The same result was obtained when we compared cell cycle time between sister RPCs that self renewed (P/D) or terminally divided (D/D division) (Fig. 4D).

The results above indicated that cell cycle time was variable and independent of the mode of RPC division or cell fate choice. Yet the cell cycle times in RPCs must influence the rate that cells are generated in the retina during development and contribute to the general timing of neurogenesis. We grouped the data from all cell divisions, independent of fate, and found that the cell cycle time was variable within the RPC population, with an average of 56.0 hours and a population standard deviation of 18.9 hours. These data were well approximated by a log-normal distribution (Fig. 5A). Also, upon comparing the cell cycle times of any consecutive divisions (n=61), we found no evidence of correlation (Fig. 5B), indicating that cell cycle time varies from one generation to the next within a lineage, although sister RPCs tended to have similar cell cycle times (see Fig. S6 in the supplementary material). Similarly, when we plotted the time at which the terminal division took place relative to the time of the previous division for each reconstructed lineage, we found no evidence of correlation (Fig. 5C), indicating that the timing of lineage termination does not depend on the time of the previous division. Consequently, RPC lineages displayed considerable variation in the number of cell generations they go through before undergoing a terminal division (Fig. 5D).

These results suggested that RPCs do not depend on mechanisms that count cell cycle time or the number of divisions to regulate lineage termination. By refining the stochastic model associated with the modes of division (defined above) to include a log-normal spectrum of division times (consistent with the experimental data), we were able to generate a theoretical distribution of lineage termination times (see Materials and methods) that showed a remarkable agreement with the overall distribution of termination times obtained experimentally (Fig. 6). Together, these results indicate that the timing of lineage termination, and thus the overall size of the retina, may be explained simply as the result of a combination of stochastic fate decisions.

Cell fate specification relies primarily on stochastic choices among available fates

Previous experiments have shown that rod photoreceptors represent 73% of all cells in the mouse retina in vivo (Young, 1985), and, similarly, 73.8% of all cells produced in the reconstructed lineages were RPh. How is such an imbalance of cell type production achieved? It could be that multipotent RPCs are largely biased toward producing photoreceptor cells at each division. Alternatively, it could be that a subset of RPCs becomes committed at some point in their lineage to generate exclusively RPh cells, thereby greatly increasing the number of RPh cells that can be produced from the same RPC pool size. Although differences may exist between in vivo and in vitro lineage progression, the continuous observation of RPC lineages performed in this study allowed us to begin to address this problem directly.

To benchmark the experimental data, we used a model in which both the balance between proliferation and differentiation, and the differentiated cell type, were chosen at random, with probabilities fixed by the measured average of each cell type produced in the clones (i.e. the probability that a differentiated cell adopts an RPh fate is given by P_{RPh}=0.738, etc.), independent of the fate of its sister, parent or any other cell in its lineage. Then, to seek evidence for lineage specification, we looked for the simplest statistical measure focusing on the correlation of cell fate between consecutive generations of cells. Specifically, we explored the correlation between the fates of two consecutive lineage-related divisions. For example, in Fig. 1E, the comparison would be between cells 1 and 2, where cell 1 divided to produce an RPC (cell 2) and an RPh, and cell 2 (always an RPC) divided to produce an Am and a Bi. In Table 2, this would be noted as (RPh, AmBi). From a total of 201 qualifying divisions from within the 129 clones, the number that generated a given cell fate versus the fate of the sister of the parent cell is shown in Table 2.

From the raw experimental data several features emerged. First, there were a number of entries for which no examples were found. Second, several of the entries were large, including the putative RPh lineage (RPh, RPhRPh) and (RPh, RPCRPh). However, by themselves, neither of these observations provides conclusive evidence for recurring lineage patterns. Since the data were acquired from only a limited number of clones, if certain lineage combinations were rare we might indeed expect to record no

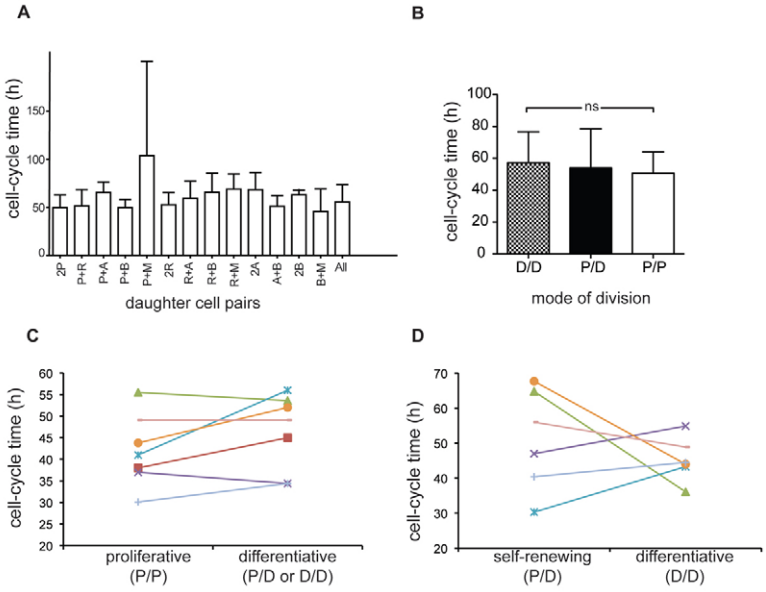

Fig. 4. Cell cycle time does not correlate with cell fate. (**A**) Average cell cycle time (mean + population s.d.) of RPCs generating all the different combinations of daughter cell pairs observed in this study. A, amacrine; B, bipolar; M, Müller; P, progenitor cell; R, rod photoreceptor. (**B**) Average cell cycle time (mean + population s.d.) of RPCs undergoing P/P, P/D or D/D divisions. ns, not significant. (**C**,**D**) Comparison of cell cycle times of sister RPCs undergoing proliferative (P/P) versus differentiative (P/D or D/D) divisions (C), or self-renewing (P/D) versus differentiative (D/D) divisions (D). Each line represents a pair of sister RPCs.

examples in the limited data set. Moreover, if cell fate choice were stochastic, but heavily biased toward RPh fate, we might find large entries in a seemingly RPh-specific lineage that derived simply by chance and not from early lineage commitment. Thus, to calibrate the data we used the stochastic model as a benchmark.

In Table 2, we also show the expected number of entries for an experiment with the same number, 201, of qualifying cell divisions if cell fate outcome were random. In addition, we have included the number of experiments (each with 201 qualifying cell divisions) that we would expect to have to perform to find at least one experiment with a statistical fluctuation that was equal to, or larger than, the actual measured experimental value. If this number is greatly in excess of the 75 possible fate outcomes in the table, we can consider the entry as an outlier, seemingly inconsistent with the random hypothesis. If, by contrast, it lies within 75, any departure of the experimental value from the expected result can be explained simply as a fluctuation associated with small-number statistics.

From this analysis, we noticed, for example, that the large entry for (RPh, RPCRPh) lies well within the expected range for the random model, along with the vast majority of other entries, consistent with such combinations being produced stochastically. However, from the 75 entries, five outliers were identified, which stand at three or more standard deviations from the expected average: (RPC, RPCRPC); (RPh, AmAm); (RPC, AmBi); (RPC, BiMu); and (Bi, AmBi). Such outliers should appear at most only once per 370 entries. Moreover, the (Bi, AmBi) entry lies beyond five standard deviations and indeed would only be expected to appear around once in 4.6 million experiments. Clearly, these

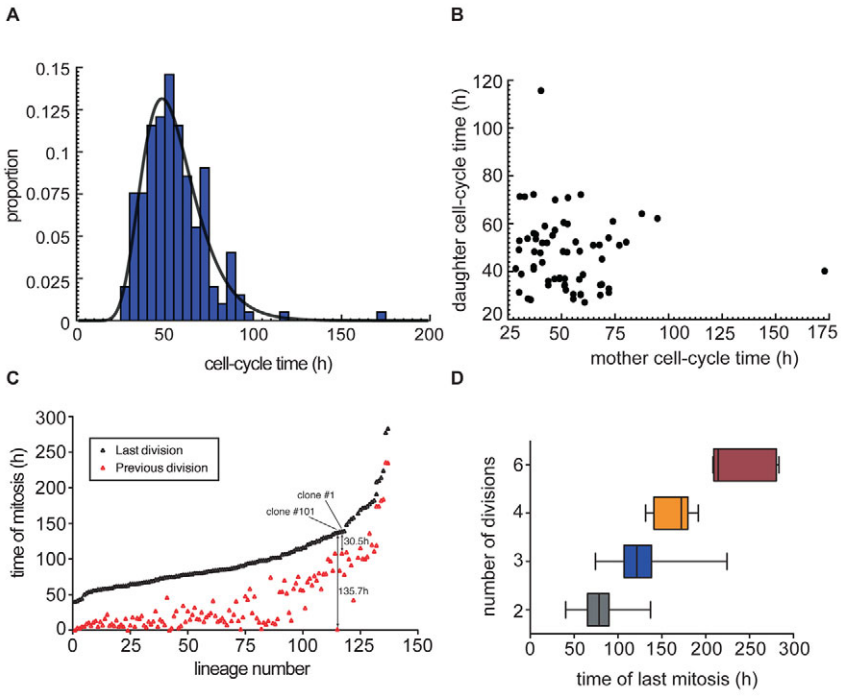

Fig. 5. Cell cycle time and number of divisions vary among RPC lineages. (**A**) Observed cell cycle time distribution (bars) together with a log-normal fit (line). The mean is 56.0 hours and population s.d. is 18.9 hours. (**B**) Cell cycle times of daughter RPCs plotted against the cell cycle times of their mothers reveals no discernable correlation. (**C**) The cell cycle time of the final two divisions of each lineage. The clones are aligned according to the cycle time of the terminal division. Note that the time of the previous mitosis is highly variable. (**D**) Larger clones can terminate their lineage before smaller clones. Note the overlap between the time of the final division in smaller and larger clones. Box plots show medians, 25% and 75% percentiles, and whiskers show minimum to maximum values.

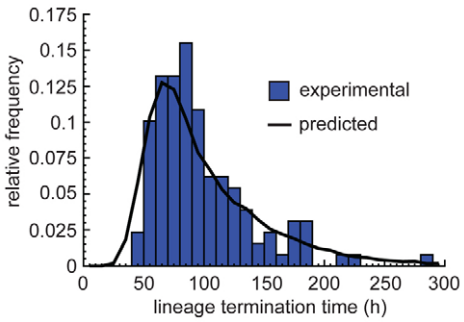

Fig. 6. A stochastic model accurately predicts the observed distribution of lineage termination times. The data (bars) show the measured distribution of lineage termination times. The line shows the predicted distribution of lineage termination times for a stochastic model in which the ratios of proliferation and differentiation are the same as that defined in Fig. 2, and the distribution of cell cycle times is taken to be log-normal with parameters chosen to fit the experimental data in Fig. 5. The curve is obtained from a Monte Carlo simulation (see Materials and methods). This comparison provides a sensitive test of the stochastic model, as deviations from it are magnified through repeated application.

cannot be explained simply as a number fluctuation, and although the chronology of cell type production might somewhat influence lineage selection, these results suggest that, in addition to stochastic mechanisms, specific recurring lineages or lineage priming may play a part in retinogenesis.

DISCUSSION

Stochastic fate characteristics of an equipotent cell population have been reported in the homeostasis of a variety of tissue stem cell populations (Clayton et al., 2007). The current study suggests that stochastic mechanisms might also operate in developing tissues and in particular the vertebrate CNS. In our view, RPC division and fate choice, at least at this stage of development, are analogous to throwing dice, in which each throw is independent of the previous one. The dice, however, might be 'loaded' or biased toward particular modes of division and cell type choices. Indeed, the loading of the dice might change over time, such that the probability of undergoing a differentiative division or of giving rise to a specific cell type is adapted to each developmental stage. Importantly, the stochasticity in cell fate choice reported here does not imply the absence of regulation. Intrinsic stochastic behaviors, such as those described here, might derive from complex regulatory machinery combined with heterogeneity in the expression of factors that influence proliferation and fate choice. Below, we discuss this model and its implications.

Order of cell birth in the retina

We find here that the order of cell birth observed at the population level is not strictly recapitulated within each lineage, at least not from E20 onwards in vitro. This finding contrasts with a recent study of clones generated in vivo in the *Xenopus* retina in which BrdU labeling provided evidence that cell genesis follows a rigid sequence of production: RGC, horizontals, cones, RPh, Am, Bi and Mu (Wong and Rapaport, 2009). The reasons why different results were obtained in the current study remains unclear, but as examples of violations to the birth order were also reported in frogs, it might be that deviations from a strict birth order within a lineage are more common in mammals. Perhaps the mechanisms regulating lineage progression in vertebrate retinas vary within species to accommodate developmental timing constraints. In the frog retina, for example, the full complement of retinal cell types develops within 2 days, whereas this process takes ~3 weeks in the rodent retina. Another simple explanation is that lineage progression in vitro does not entirely reflect the in vivo situation, but the finding that the general order of cell birth in vitro is reproduced at the population level argues against this possibility.

Although it was known that RPCs could give rise to a neuron and a Mu cell up until the final division (Turner and Cepko, 1987), we now provide direct evidence that RPCs can generate neurons, even after they have produced glial cells within the same lineage. Since Mu cells can be triggered to re-enter the cell cycle and generate new neurons (Fischer and Reh, 2001; Fischer and Reh, 2003; Karl et al., 2008), it is tempting to speculate that self-

Table 2. Comparison of fate characteristics between consecutive cell generation outcomes against a purely stochastic model of differentiation

	2×RPC	RPC RPh	RPC Am	RPC Bi	RPC Mu	2×RPh	RPh Am	RPh Bi	RPh Mu	2×Am	Am Bi	Am Mu	2×Bi	Bi Mu	2×Mu
RPC	$7^{2.2}_{512}$	$9^{6.6}_{4}$	$0^{0.9}_{1}$	$1^{1.1}_{1}$	$0^{0.3}_{1}$	$9^{15.8}_{15}$	$3^{4.6}_{2}$	$2^{5.5}_{7}$	$0^{1.2}_{2}$	$1^{0.3}_{23}$	$4^{0.8}_{784}$	$0^{0.2}_{1}$	$1^{0.5}_{12}$	$2^{0.2}_{777}$	$0^{0.0}_{1}$
RPh	$3^{6.6}_{6}$	$24^{19.4}_{4}$	$3^{2.8}_{2}$	$1^{3.4}_{5}$	$1^{0.7}_{6}$	$63^{46.8}_{135}$	$9^{13.4}_{5}$	$10^{16.2}_{10}$	$5^{3.6}_{4}$	$5^{1.0}_{2121}$	$3^{2.3}_{3}$	$0^{0.5}_{1}$	$3^{1.4}_{19}$	$1^{0.6}_{8}$	$0^{0.1}_{1}$
Am	$1^{0.9}_{4}$	$1^{2.8}_{3}$	$0^{0.4}_{1}$	$1^{0.5}_{12}$	$0^{0.1}_{1}$	$4^{6.7}_{3}$	$0^{1.9}_{5}$	$0^{2.3}_{8}$	$1^{0.5}_{11}$	$0^{0.1}_{1}$	$0^{0.3}_{1}$	$0^{0.1}_{1}$	$0^{0.2}_{1}$	$0^{0.1}_{1}$	$0^{0.0}_{1}$
Bi	$0^{1.1}_{2}$	$0^{3.4}_{18}$	$0^{0.5}_{1}$	$0^{0.6}_{1}$	$1^{0.1}_{134}$	$9^{8.1}_{2}$	$3^{2.3}_{3}$	$0^{2.8}_{12}$	$1^{0.6}_{8}$	$0^{0.2}_{1}$	$6^{0.4}_{4592680}$	$0^{0.1}_{1}$	$0^{0.2}_{1}$	$1^{0.1}_{189}$	$0^{0.0}_{1}$
Mu	$0^{0.3}_{1}$	$1^{0.7}_{6}$	$0^{0.1}_{1}$	$0^{0.1}_{1}$	$0^{0.0}_{1}$	$1^{1.8}_{1}$	$0^{0.5}_{1}$	$0^{0.6}_{1}$	$0^{0.1}_{1}$	$0^{0.0}_{1}$	$0^{0.1}_{1}$	$0^{0.0}_{1}$	$0^{0.1}_{1}$	$0^{0.0}_{1}$	$0^{0.0}_{1}$

Each entry displays three quantities for a given triplet of cells generated by two consecutive lineage-related divisions. The nomenclature is illustrated by the example in Fig. 1E, where the comparison is between the outcome of division for cells 1 and 2. In total, among the 129 clones, 201 such events were observed. The number in a large font denotes the observed frequency of the event. The superscript represents the prediction made by a stochastic model in which the relative division probabilities leading to proliferation and differentiation are set by the parameters shown in Fig. 2, and the relative probabilities of the differentiated cell types is specified at random with P_{RPh}=0.738, P_{Bi}=0.128, P_{Am}=0.106 and P_{Mu}=0.028, corresponding to the observed frequencies of the population (see Materials and methods). The subscript indicates the quality of the agreement between the experiment and the stochastic model, expressed as the number of experiments (each involving 201 aunt/niece triplets) one would expect to perform before seeing a statistical fluctuation of this magnitude or greater. This figure should be compared with the total number of entries (75) – much greater than this is a sign of a genuine outlier. Outliers that stand at three and four standard deviations are light and dark grey, respectively. For example, the entry at (RPh, RPCRPh) represents events involving two consecutive P/D divisions in which both differentiated progeny adopted the RPh cell fate. Out of the 201 entries, from the table, we find that such an event occurred 24 times. This compares to the 19.4 average predicted by the stochastic model. From the subscripted number, we see that one would expect to see a departure from the theoretical prediction of this magnitude or larger in one out of four experiments owing to statistical fluctuations, i.e. the observed data are entirely compatible with the statistical model. By contrast, if we look at the entry (Bi, AmBi), we expect to see an average of 0.4 events out of 201, whereas the data show six. Such a fluctuation would arise in typically only one out of 4.6 million experiments, i.e. the observed data are clearly incompatible with the statistical model as defined.

renewing RPCs that generate a Mu cell and another RPC might be able to transmit neurogenic potential to the Mu daughter cell, whereas terminally dividing RPCs could not.

Balancing proliferation and differentiation

One of the most striking results in this study is that the variability of clone size is well described by a model in which RPCs stochastically choose between P/P, P/D and D/D modes of division according to a fixed ratio that does not appear to evolve over time or depend on lineage history. It is important to note, however, that we are looking at RPCs at E20 in vitro, near the end of retinogenesis. At early stages of retinal development in vivo, all RPCs remain in the cell cycle, so all RPCs initially divide with only P/P divisions. At some point in retinogenesis (~E13), the first terminally differentiating daughters arise. It thus seems that individual RPCs shift their ratio of P/P, P/D and D/D divisions over time, although whether this is intrinsically programmed or a function of extrinsic influences, such as growth factors, has not yet been tested. A cell-intrinsic timer model has been proposed for oligodendrocyte precursor cells (OPCs) that involves p27Kip1 (Cdkn1b) and Id4 (Raff, 2007). Components of the intrinsic OPC timer might play a role in the retina, as *p27Kip1* knockout mice are ~30% larger than their wild-type counterparts and have increase cell numbers in all their organs, including the retina (Nakayama et al., 1996; Fero et al., 1996; Kiyokawa et al., 1996; Tokumoto et al., 2002). In addition, secreted feedback inhibitory signals, such as Shh and Gdf11, which are known to regulate RPC proliferation and RGC production (Kim et al., 2005; Wang et al., 2005), could operate to change the ratio of P/P, P/D and D/D divisions over time. It will be interesting to test whether the addition of such factors to clonal-density cultures changes the ratio of cell division modes.

Timing the completion of a lineage

Our data show that cell cycle times are highly variable and follow an approximately log-normal distribution in which consecutive cell cycle times remain largely uncorrelated. Intriguingly, however, the cell cycle time of sister RPCs that both continue to divide appears to exhibit a degree of synchronization (see Fig. S6 in the supplementary material), suggesting that a mother RPC might be able to pass on cell cycle information to its daughter cells, thereby contributing to the timing of lineage termination. Such synchronous divisions of sister progenitor cells have also been reported for cortical progenitors, OPCs and even zebrafish RPCs (Baye and Link, 2007; Gao et al., 1997; Qian et al., 1998; Qian et al., 2000), suggesting that it might be a general process involved in timing lineage progression in the CNS. In addition to variable cell cycle times, we find that the number of rounds of cell division that a given RPC goes through before undergoing terminal differentiation is variable from one lineage to another, even for two lineages that terminate in the same developmental time window. Together, these results suggest that RPCs are not counting cell cycle time or rounds of division to coordinate when to exit the cell cycle and differentiate, much like what was proposed in the OPC timer model (Gao et al., 1997; Raff, 2007).

Remarkably, when we factor in the observed variability of cell cycle times in the stochastic model, we find that the distribution of lineage termination times predicted by the model accurately reproduces the experimental data. Since the ratio of P/P, P/D and D/D divisions clearly influences the chance that a particular RPC lineage will terminate or continue to progress in time, a better understanding of the factors that affect the cell division mode ratio will help to elucidate the molecular mechanisms of the stochastic model.

Cell type composition in retinal clones: stochastic decisions versus predetermined lineages

Pioneering cell lineage-tracing experiments in vivo have shown that RPCs generate a large variety of clones, some containing only one cell type and others containing as many as seven different cell types (Holt et al., 1988; Turner and Cepko, 1987; Turner et al., 1990; Wetts and Fraser, 1988). These studies led to the widely accepted model that RPCs are initially multipotent and then go through a series of developmental phases called ‘competence states’, in which they progressively lose the ability to generate specific cell types and acquire the competence to generate others (Cepko et al., 1996; Livesey and Cepko, 2001). Our current findings indicate that, within a particular temporal competence stage near the end of retinogenesis when only RPh, Bi, Am and Mu cells are being produced, the vast majority of cell compositions observed in the clones can be explained on the basis of stochastic cell fate choice according to the ratios of these cell types observed in the mature retina. Some lineages are more commonly observed, such as the RPh-only lineage. We find a total of 57 RPh-only lineages out of the 129 lineages analyzed, and 55 out of 57 are generated through P/D divisions followed by a D/D division. Although such lineages might appear predetermined and generated by an RPh-committed precursor, the frequency of such lineages is actually expected from stochastic decisions biased by the abundance of RPh cells produced in the total population of cells and the predominance of P/D and D/D divisions at this stage of retinogenesis.

These results suggest that the assignment of cell fate operates independently of cell cycle regulation, mode of division or lineage history. Consistent with this conclusion, we recently reported that Ikaros, a zinc-finger transcription factor, is apparently necessary and sufficient to confer early temporal competence to RPCs independently of cell proliferation (Elliott et al., 2008). In gain-of-function experiments, for example, Ikaros was found to be sufficient to confer the competence to generate early-born retinal cell types in RPCs, but did not affect their proliferation capacity. Similarly, it has been shown that when specific cell type determinants, such as Ptf1a (which specifies all the inhibitory cells in the retina), are knocked out, cells just switch from one type of neuron to another, without affecting proliferation (Dullin et al., 2007; Fujitani et al., 2006).

Recently, we showed that mathematical analysis of RPC behavior in culture could predict the outcome of the following division, suggesting that RPCs may be committed to specific fates before they undergo mitosis (Cohen et al., 2010). This might seem inconsistent with the stochastic model proposed in this study, but taking both sets of observations together, they suggest that many of the stochastic decisions might actually be made just before mitosis (e.g. in G2).

It must be emphasized, however, that not all our results are consistent with the proposed stochastic model. In particular, a small proportion of RPCs appear to generate particular combinations of cell types that occur at frequencies that are very unlikely according to the stochastic assumptions. Although the observed number of such combinations is small, it is interesting to consider the possibility that some RPCs become primed early on to generate a particular combination of cell types. Such priming could take place very late in a lineage, as is the case with that specified by Ath5

(Atoh7 – Zebrafish Information Network), which is expressed in a subset of RPCs in zebrafish at G2 of the final cell division, and which accounts for the likelihood that one daughter will become an RGC whereas the other will become a photoreceptor, horizontal or Am cell, but not a Bi or Mu (Poggi et al., 2005), the latter cell types deriving from the subset of progenitors that express Vsx1 or Vsx2 but not Ath5 (Vitorino et al., 2009). One thus expects some degree of molecular heterogeneity in the RPC population, which is also supported by recent single-cell gene expression profiling in mouse RPCs (Trimarchi et al., 2008).

Acknowledgements
We thank Andrew Cohen for providing lineage drawing software; Christine Jolicoeur for technical support; Jessica Barthe for managing the animal colony; Martin Raff for critically reading the manuscript; and members of the M.C. lab for ongoing discussions about this project. This work was supported by grants from the Canadian Institutes of Health Research (MOP 77570) and the Foundation Fighting Blindness – Canada (to M.C.), the Wellcome Trust (to W.A.H.) and the UK Engineering and Physical Sciences Research Council (to B.D.S.). M.C. is a W. K. Stell Scholar of the Foundation Fighting Blindness – Canada. Deposited in PMC for release after 6 months.

Competing interests statement
The authors declare no competing financial interests.

Supplementary material
Supplementary material for this article is available at
http://dev.biologists.org/lookup/suppl/doi:10.1242/dev.059683/-/DC1

References

Baye, L. and Link, B. (2007). Interkinetic nuclear migration and the selection of neurogenic cell divisions during vertebrate retinogenesis. *J. Neurosci.* **27**, 10143-10152.
Cayouette, M., Barres, B. A. and Raff, M. (2003). Importance of intrinsic mechanisms in cell fate decisions in the developing rat retina. *Neuron* **40**, 897-904.
Cayouette, M., Poggi, L. and Harris, W. A. (2006). Lineage in the vertebrate retina. *Trends Neurosci.* **29**, 563-570.
Cepko, C. L., Austin, C. P., Yang, X., Alexiades, M. and Ezzeddine, D. (1996). Cell fate determination in the vertebrate retina. *Proc. Natl. Acad. Sci. USA* **93**, 589-595.
Clayton, E., Doupe, D. P., Klein, A. M., Winton, D. J., Simons, B. D. and Jones, P. H. (2007). A single type of progenitor cell maintains normal epidermis. *Nature* **446**, 185-189.
Cohen, A. R., Gomes, F. L. A. F., Roysam, B. and Cayouette, M. (2010). Computational prediction of neural progenitor cell fates. *Nat. Methods* **7**, 213-218.
Dullin, J. P., Locker, M., Robach, M., Henningfeld, K. A., Parain, K., Afelik, S., Pieler, T. and Perron, M. (2007). Ptf1a triggers GABAergic neuronal cell fates in the retina. *BMC Dev. Biol.* **7**, 110.
Elliott, J., Jolicoeur, C., Ramamurthy, V. and Cayouette, M. (2008). Ikaros confers early temporal competence to mouse retinal progenitor cells. *Neuron* **60**, 26-39.
Fero, M. L., Rivkin, M., Tasch, M., Porter, P., Carow, C. E., Firpo, E., Polyak, K., Tsai, L. H., Broudy, V., Perlmutter, R. M. et al. (1996). A syndrome of multiorgan hyperplasia with features of gigantism, tumorigenesis, and female sterility in p27(Kip1)-deficient mice. *Cell* **85**, 733-744.
Fischer, A. J. and Reh, T. A. (2001). Muller glia are a potential source of neural regeneration in the postnatal chicken retina. *Nat. Neurosci.* **4**, 247-252.
Fischer, A. J. and Reh, T. A. (2003). Potential of Muller glia to become neurogenic retinal progenitor cells. *Glia* **43**, 70-76.
Fujitani, Y., Fujitani, S., Luo, H., Qiu, F., Burlison, J., Long, Q., Kawaguchi, Y., Edlund, H., MacDonald, R. J., Furukawa, T. et al. (2006). Ptf1a determines horizontal and amacrine cell fates during mouse retinal development. *Development* **133**, 4439-4450.
Gao, F. B., Durand, B. and Raff, M. (1997). Oligodendrocyte precursor cells count time but not cell divisions before differentiation. *Curr. Biol.* **7**, 152-155.
Gaspard, N., Bouschet, T., Hourez, R., Dimidschstein, J., Naeije, G., van den Ameele, J., Espuny-Camacho, I., Herpoel, A., Passante, L., Schiffmann, S. N. et al. (2008). An intrinsic mechanism of corticogenesis from embryonic stem cells. *Nature* **455**, 351-357.
Gillespie, D. T. (1977). Exact stochastic simulation of coupled chemical reactions. *J. Phys. Chem.* **81**, 2340-2361.
Holt, C. E., Bertsch, T. W., Ellis, H. M. and Harris, W. A. (1988). Cellular determination in the Xenopus retina is independent of lineage and birth date. *Neuron* **1**, 15-26.
Kao, C. F. and Lee, T. (2010). Birth time/order-dependent neuron type specification. *Curr. Opin. Neurobiol.* **20**, 14-21.
Karl, M. O., Hayes, S., Nelson, B. R., Tan, K., Buckingham, B. and Reh, T. A. (2008). Stimulation of neural regeneration in the mouse retina. *Proc. Natl. Acad. Sci. USA* **105**, 19508-19513.
Kim, J., Wu, H. H., Lander, A. D., Lyons, K. M., Matzuk, M. M. and Calof, A. L. (2005). GDF11 controls the timing of progenitor cell competence in developing retina. *Science* **308**, 1927-1930.
Kiyokawa, H., Kineman, R. D., Manova-Todorova, K. O., Soares, V. C., Hoffman, E. S., Ono, M., Khanam, D., Hayday, A. C., Frohman, L. A. and Koff, A. (1996). Enhanced growth of mice lacking the cyclin-dependent kinase inhibitor function of p27(Kip1). *Cell* **85**, 721-732.
Livesey, F. J. and Cepko, C. L. (2001). Vertebrate neural cell-fate determination: lessons from the retina. *Nat. Rev. Neurosci.* **2**, 109-118.
Nakayama, K., Ishida, N., Shirane, M., Inomata, A., Inoue, T., Shishido, N., Horii, I. and Loh, D. Y. (1996). Mice lacking p27(Kip1) display increased body size, multiple organ hyperplasia, retinal dysplasia, and pituitary tumors. *Cell* **85**, 707-720.
Poggi, L., Vitorino, M., Masai, I. and Harris, W. A. (2005). Influences on neural lineage and mode of division in the zebrafish retina in vivo. *J. Cell Biol.* **171**, 991-999.
Price, J., Williams, B. and Grove, E. (1991). Cell lineage in the cerebral cortex. *Development* **Suppl. 2**, 23-28.
Qian, X., Goderie, S. K., Shen, Q., Stern, J. H. and Temple, S. (1998). Intrinsic programs of patterned cell lineages in isolated vertebrate CNS ventricular zone cells. *Development* **125**, 3143-3152.
Qian, X., Shen, Q., Goderie, S. K., He, W., Capela, A., Davis, A. A. and Temple, S. (2000). Timing of CNS cell generation: a programmed sequence of neuron and glial cell production from isolated murine cortical stem cells. *Neuron* **28**, 69-80.
Raff, M. (2007). Intracellular developmental timers. *Cold Spring Harbor Symp. Quant. Biol.* **72**, 431-435.
Rapaport, D. H., Wong, L. L., Wood, E. D., Yasumura, D. and LaVail, M. M. (2004). Timing and topography of cell genesis in the rat retina. *J. Comp. Neurol.* **474**, 304-324.
Reid, C. B., Tavazoie, S. F. and Walsh, C. A. (1997). Clonal dispersion and evidence for asymmetric cell division in ferret cortex. *Development* **124**, 2441-2450.
Rose, L. S. and Kemphues, K. J. (1998). Early patterning of the C. elegans embryo. *Annu. Rev. Genet.* **32**, 521-545.
Shen, Q., Wang, Y., Dimos, J. T., Fasano, C. A., Phoenix, T. N., Lemischka, I. R., Ivanova, N. B., Stifani, S., Morrisey, E. E. and Temple, S. (2006). The timing of cortical neurogenesis is encoded within lineages of individual progenitor cells. *Nat. Neurosci.* **9**, 743-751.
Slater, J. L., Landman, K. A., Hughes, B. D., Shen, Q. and Temple, S. (2009). Cell lineage tree models of neurogenesis. *J. Theor. Biol.* **256**, 164-179.
Sulston, J. E. and Horvitz, H. R. (1977). Post-embryonic cell lineages of the nematode, Caenorhabditis elegans. *Dev. Biol.* **56**, 110-156.
Sulston, J. E., Schierenberg, E., White, J. G. and Thomson, J. N. (1983). The embryonic cell lineage of the nematode Caenorhabditis elegans. *Dev. Biol.* **100**, 64-119.
Tokumoto, Y. M., Apperly, J. A., Gao, F. B. and Raff, M. C. (2002). Posttranscriptional regulation of p18 and p27 Cdk inhibitor proteins and the timing of oligodendrocyte differentiation. *Dev. Biol.* **245**, 224-234.
Trimarchi, J. M., Stadler, M. B. and Cepko, C. L. (2008). Individual retinal progenitor cells display extensive heterogeneity of gene expression. *PLoS ONE* **3**, e1588.
Turner, D. L. and Cepko, C. L. (1987). A common progenitor for neurons and glia persists in rat retina late in development. *Nature* **328**, 131-136.
Turner, D. L., Snyder, E. Y. and Cepko, C. L. (1990). Lineage-independent determination of cell type in the embryonic mouse retina. *Neuron* **4**, 833-845.
Vitorino, M., Jusuf, P. R., Maurus, D., Kimura, Y., Higashijima, S. and Harris, W. A. (2009). Vsx2 in the zebrafish retina: restricted lineages through derepression. *Neural Dev.* **4**, 14.
Walsh, C. and Cepko, C. L. (1990). Cell lineage and cell migration in the developing cerebral cortex. *Experientia* **46**, 940-947.
Wang, Y., Dakubo, G. D., Thurig, S., Mazerolle, C. J. and Wallace, V. A. (2005). Retinal ganglion cell-derived sonic hedgehog locally controls proliferation and the timing of RGC development in the embryonic mouse retina. *Development* **132**, 5103-5113.
Wetts, R. and Fraser, S. E. (1988). Multipotent precursors can give rise to all major cell types of the frog retina. *Science* **239**, 1142-1145.
Wong, L. L. and Rapaport, D. H. (2009). Defining retinal progenitor cell competence in Xenopus laevis by clonal analysis. *Development* **136**, 1707-1715.
Young, R. W. (1985). Cell differentiation in the retina of the mouse. *Anat. Rec.* **212**, 199-205.